Quantum Computing with Electrons Floating on Liquid Helium

P. M. Platzman[1]* and M. I. Dykman[2]

A quasi–two-dimensional set of electrons ($1 < N < 10^9$) in vacuum, trapped in one-dimensional hydrogenic levels above a micrometer-thick film of liquid helium, is proposed as an easily manipulated strongly interacting set of quantum bits. Individual electrons are laterally confined by micrometer-sized metal pads below the helium. Information is stored in the lowest hydrogenic levels. With electric fields, at temperatures of 10^{-2} kelvin, changes in the wave function can be made in nanoseconds. Wave function coherence times are 0.1 millisecond. The wave function is read out with an inverted dc voltage, which releases excited electrons from the surface.

There is much interest in constructing analog quantum computers (AQC). Such objects would solve problems that could never be solved by any classical digital computer, even ones that were hundreds of billions of times larger and faster than current ones (*1, 2*). An AQC is made up of N interacting quantum objects called quantum bits (qubits), which have at least two quantum states (*3*). Unlike their classical counterparts, which have states of only 1 or 0 (up or down), qubits can be in a complex linear superposition of both states until they are finally read out.

Initially, the qubits are in some particular set of states (initial wave function ψ_0) representing the input data. The qubits are then allowed to interact and evolve in time under the action of some possibly time-dependent Hamiltonian. The Hamiltonian can be thought of as the program. After some time t_f, the wave function ψ_f contains, in probabilistic terms, the answer to "the computation."

Finding the algorithm (the time-dependent Hamiltonian) is a real challenge, and only a few have been found (*4, 5*). However, finding physical systems that are suitable for meaningful quantum computation is a more difficult problem because these physical systems must consist of interacting quantum objects ($N \geq 10^3$) whose interactions and states can be conveniently manipulated. In addition, the qubits must be sufficiently isolated from the outside world (other degrees of freedom) so that interaction with such reservoirs does not disturb the time-dependent aspects of the computational wave function (*3*). Atoms in traps (*6*), cavity quantum electrodynamic systems (*7*), nuclei in complex molecules (*8*), quantum dots (*9*), and nuclear spins of atoms in doped silicon devices have been proposed (*10*). For these systems, almost insurmountable technological and scientific barriers exist, which must be overcome to achieve a useful quantum computer.

Here, we suggest using a set of electrons ($1 < N < 10^9$) trapped in vacuum at a low-temperature liquid-helium interface for implementing a large AQC. Much of the basic physics we present here is already well documented (*11*). However, what we show for the first time is that under realistically obtainable conditions (that is, correct geometry, temperature, magnetic field, and so forth), these quasi–two-dimensional (2D) electrons can behave as an AQC with many qubits. In addition to the suggested "system design," we have carefully calculated the very important decoherence effects to show that they are acceptably small.

A single electron on a bulk film of thickness $d \geq 0.5$ μm is weakly attracted and trapped by an image potential of the form $V = \Lambda e^2/z$, where e is the charge on the electron and z is the coordinate of the electrons perpendicular to the interface (Fig. 1) (*11*). In this case, $\Lambda \equiv (\varepsilon - 1)/4(\varepsilon + 1) \cong 0.01$, because $\varepsilon \cong 1.057$ is the dielectric constant of liquid helium. Because there is a barrier of 1 eV for penetration into the helium, the electrons' z motion is described by a 1D hydrogenic spectrum; that is, the mth state has an energy $E_m = -R/m^2$ with an effective Rydberg energy $R = \Lambda^2 e^4 m_e/2\hbar^2 \cong 8$ K and an effective Bohr radius $r_B = \hbar^2/(m_e e^2 \Lambda) \cong 76$ Å (*12*), where $\hbar$ is Planck's constant divided by 2π.

Below a temperature $T_\lambda = 2.2$ K, He^4 is a superfluid with a mass density ρ and surface tension σ. For $T < 0.1$ K, the vapor pressure of helium atoms above the liquid is zero, so that the only substantial electron coupling to the outside world is to thermally excited height variations $\delta(\mathbf{r}, t)$ of the helium surface, where $\mathbf{r}$ is the electron in-plane coordinate and t is time. The height variations of the surface are described as propagating capillary waves having a dispersion relation $\omega^2 = (\sigma/\rho)k^3$ (*11*) and a coupling Hamiltonian $H_{er} = e\mathcal{E}_T\delta$, where $\mathcal{E}_T$ is the total z-directed electric field on the electron. For wave vectors $k < 5 \times 10^5$ cm^{-1}, $\omega < 4 \times 10^{-3}$ K so that, at 10^{-2} K, many ripplons are present, and the average mean-square displacement of the surface is $\delta_T \equiv (k_B T/\sigma)^{1/2} \cong 2 \times 10^{-9}$ cm.

In the lowest hydrogenic level, it is the weak coupling to the ripplons that limits the mobility μ of the surface-state electrons, which can be greater than 10^8 cm^2 V^{-1} s^{-1} (*13*). Additionally, the coupling to the ripplons with wave vectors $k_B \cong r_B^{-1}$ give rise to a relaxation time T_1 from the $m = 2$ to the $m = 1$ Rydberg state. A simple calculation shows that

$$\frac{\hbar}{T_1} \cong R\left(\frac{\delta_T}{r_B}\right)^2 \quad (1)$$

Because $(\delta_T/r_B) \cong 10^{-3}$, the rate $1/T_1$ is 10^{-6} of the transition frequency, ~120 GHz. This suggests that we can use the lowest two hydrogenic levels of an individual electron as a convenient qubit, whose state can be changed by the application of a microwave field. For microwave fields of a magnitude $E_{RF} \cong 1$ V cm^{-1}, the Rabi frequency $\Omega \equiv eE_{RF}r_B$, the rate at which we can switch our qubit from the lowest state to the first excited state (*14*), is $\sim 10^9$ s^{-1}. Thus, a laterally unconfined electron has an $\Omega T_1 \geq 10^4$.

For many qubits, we covered a helium layer of a thickness d of several square centimeters in area with an interacting fluid ($n_e \cong 4 \times 10^8$ cm^{-2}) of electrons $n_e \cong d^{-2}$ (*11, 12*). This was done by charging the surface with a filament in a parallel plate capacitor that was partially filled with liquid helium (Fig. 2A). The capacitor has a voltage across it, which, for a fixed geometry, determines the charge density. The pressing field $\mathcal{E}_-$ effectively acts as a uniform compensating background of charge and has a minimum value of $\mathcal{E}_- \geq 100$ V cm^{-1} for $n_e \cong 10^8$ cm^{-2}. The field $\mathcal{E}_-$ Stark shifts our hydrogenic energy levels by ~1 GHz for each volt per centimeter. It also increases the effective coupling to the ripplons. However, for $\mathcal{E}_- \cong 100$ V cm^{-1}, because the image field is $\sim 10^3$ V cm^{-1}, our estimate of T_1 is still accurate.

Because the Coulomb energy between pairs of electrons $e^2/d \cong 20$ K $\gg k_B T$, it is well known that the 2D electrons on the surface will freeze into a 2D electron solid with lattice constant $a \cong d$ (*15*). If we pattern the bottom electrode with features spaced by d (Fig. 2B), each electrode will trap one electron. In this case, each electron finds itself in an externally created potential well whose detailed shape depends on the precise

[1]Bell Laboratories, Lucent Technologies, Murray Hill, NJ 07974, USA. [2]Michigan State University, Department of Physics and Astronomy, East Lansing, MI 48824, USA.

*To whom correspondence should be addressed. E-mail: pmp@bell-labs.com

geometry and on the difference of the voltage $\delta\mathbf{V} \equiv \mathbf{V}_1 - \mathbf{V}_2$ between neighboring electrodes. This in-plane potential gives rise to a set of in-plane quantum energy levels with a spacing $\hbar\Omega_{\|} \cong [\hbar^2\pi^2/md^2(e\delta\mathbf{V}'e^{-\pi})]^{1/2}$, where $\delta\mathbf{V}'$ is the maximum of $\delta\mathbf{V}$ or $(e/d)e^{-\pi}$, as well as a Stark shift of the Rydberg states by $\Delta E = \pi e^{-\pi}\delta\mathbf{V}(r_B/d)$. For $\delta\mathbf{V} = 10^{-3}$ V, $\Omega_{\|} \cong 1.7 \times 10^{-1}$ K and $\Delta E \cong 10^{-2}$ K. Such quantization suppresses ripplon-induced decay from the excited to ground Rydberg state. We can completely eliminate this one-ripplon process if we apply a strong perpendicular magnetic field $B_\perp$. The magnetic field confines the electron to a length $\ell = (\hbar c/eB_\perp)^{1/2}$, where c is the velocity of light, and opens up gaps in the in-plane excitation spectrum of the many-electron system. This spectrum now consists of a discrete broadened ladder with spacing $\hbar\omega_c = \hbar eB_\perp/mc$ and width $\omega_{ZB} \cong (2\pi e^2/d^3m_e)(1/\omega_c)$. For $d = 0.5$ μm, $B_\perp = 1.5$ T, $\ell = 210$ Å, $\omega_c = 2$ K, and $\omega_{ZB} \cong 0.4$ K. Because the one-ripplon decay involves emission of ripplons of wave vector $k_\ell \cong \ell^{-1}$ and frequency $\omega_\ell \leq 10^{-2}$ K, it is impossible to conserve energy. In this case, the limiting linewidth is determined by a two-ripplon process, which either allows for real decay of the excited state, which is extremely slow, or an incoherent phase modulation by a quasi-elastic scattering of thermally excited ripplons with wave vectors k_ℓ (*16*), which results in a linewidth

$$\frac{1}{T_2} \cong R\left(\frac{\delta_T}{r_B}\right)^4\left(\frac{r_B}{\ell}\right)^8\frac{R^3}{\omega_{ZB}^2\omega_\ell} \qquad (2)$$

For $T = 10^{-2}$ K, $T_2 \cong 10^{-4}$ s and $\Omega T_2 \cong 10^5$.

The sudden transition from $m = 1$ to $m = 2$ will consist of a sharp no-ripplon line and, in our case, a one-ripplon side band. A calculation of the fractional intensity G in this one-ripplon side band shows that $G \cong (R^2/\omega_\ell^2)\,(\delta_T^2 r_B^2/\ell^4)\,[1/2(2\pi)^{1/2}]$. For $T = 10^{-2}$ K, $G \cong 0.05$, and the intensity is almost all in the zero-ripplon line with a weak one-ripplon continuum. The one-ripplon piece will have a width of about $\omega_\ell \cong 4 \times 10^{-3}$ K.

For two electrons near their respective electrodes, the part of the Coulomb interaction that effects the z motion is very well approximated by

$$\mathbf{V}_c(z_1, z_2) \cong \frac{e^2}{d^3}(z_1z_2) \qquad (3)$$

At $d = 0.5$ μm, this Coulomb interaction has two important features: (i) It effects a state-dependent shift of the energy of a neighbor by $\sim 10^{-2}$ K, and (ii) it allows for the coherent resonant energy transfer of excitation from one electron to another. Suppose we start with two weakly coupled nonresonant electrons (see Fig. 2 with $\mathbf{V}_1 \neq \mathbf{V}_2$) in their ground states. Because the resonant frequencies of each bit can be controlled by the voltage on the patterned electrode, a uniform microwave driving field can address any specific bit if the correct frequency is chosen. Therefore, a short pulse of radiation at the resonant frequency of the first electron puts it in the excited state. Next, sweep $\mathbf{V}_2$ so that the two levels pass through resonance and then out of resonance. If the pulse duration $T_p \cong \langle\mathbf{V}_c\rangle^{-1} \cong \Omega^{-1} \cong 10^{-2}$ K is suitably tailored, the second particle ends up in a linear superposition of ground and excited states.

The interaction between electrons (Eq. 3) will, of course, have small correction terms, which will depend on the in-plane displacements δr of the electrons from their equilibrium position, that is, $\delta\mathbf{V}(r_1, r_2, z_1, z_2) \cong \mathbf{V}_c(z_1, z_2)(\delta r_1 - \delta r_2)^2/d^2$. Such terms couple to the in-plane degrees of freedom of the two carriers. These vibrational degrees of freedom have an energy scale characterized by ω_{ZB}. This relatively high in-plane energy excitation is easily suppressed at the 10^{-6} level because of the time dependence of the pulse $T_p^{-1} \leq 1$ GHz and because $(\delta r_1 - \delta r_2)^2/d^2 \leq 10^{-3}$.

Other types of very weak dissipative processes can be present, but they are not important. More specifically, (i) spontaneous radiative emission is negligible, (ii) nonradiative decay due to pair creation in the electrodes can be completely suppressed by using superconducting electrodes with a gap greater then the transition frequency, and (iii) applying wide-band pulses with a specific time dependence will introduce voltage noise. However, assuming that these pulses are carried on a transmission line with a resistance of 50 ohms and a noise temperature of 10 K, then the capacitative plates (our electrodes) will be subject to a noise voltage of $\sim 10^{-10}$ V Hz$^{-1/2}$. For a bandwidth of 10^8 to 10^9 Hz, this implies a voltage fluctuation (noise) of $\sim 10^{-6}$ V, which is acceptable.

In order to read out the wave function at some time t_F, when the computation is completed, we apply a reverse field $\mathcal{E}_+$ to the capacitor, which would (if it were large enough) remove all the electrons from the helium surface. However, if the reverse field at the electron layer is not too strong, the electrons see a potential that has a maximum similar to that shown in Fig. 3 (*17*). For this potential, the electron tunneling rate depends exponentially on the barrier height E_{Bm}. The electrons will leave the surface in some time t_m, which is a strong function of the state m. It is possible to set the field $\mathcal{E}_+$ so that if one waits for some reasonable time, say 1 μs, only the excited electrons will come off. They will arrive at the plate (anode) with some modest kinetic energy, that is, tens of electron volts. If the anode is part of a low-temperature channel plate arrangement with a spatial resolution of 1 μm or less, those electrons may be imaged, and a "picture" is taken of the wave function. Another possibility is to measure the change of voltage on the patterned electrodes, which is about $e^2/d \cong 1$ meV.

Two-dimensional electrons on helium are a unique system in the context of very large

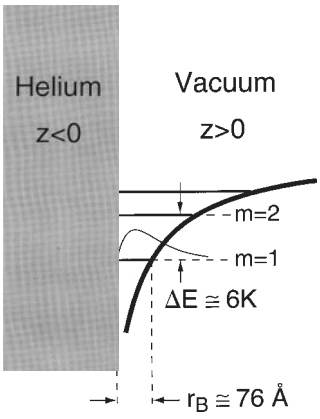

Fig. 1. The geometry for an electron trapped at the helium vacuum interface. The Rydberg energy levels along with a typical $m = 1$ wave function are displayed in the image potential $V(z) = -\Lambda e^2/z$ for $z > 0$.

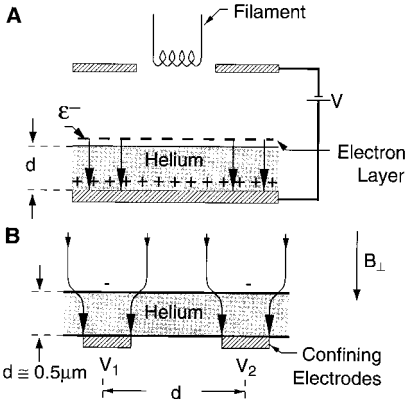

Fig. 2. (**A**) The parallel plate capacitor arrangement for confining a uniform layer of electrons. The holding field $\mathcal{E}_-$ and the filament for charging are shown. (**B**) The geometry for a pair of electrons on a patterned substrate. The rough dimensions, the shape of the field lines, and the control gate are included.

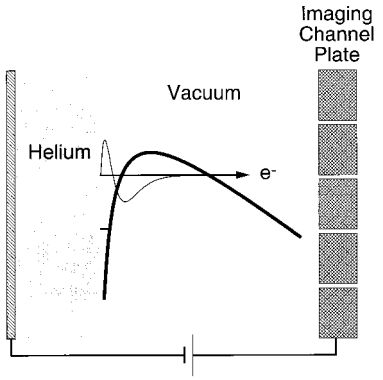

Fig. 3. The read-out configuration. The potential leading to tunneling when a reverse field is shown, along with a schematic of the position-sensitive channel plate.

AQC systems. They are scalable, easily manipulated, and have perfectly acceptable decoherence times, and no existing technological barriers seem to be present.

References and Notes

1. R. P. Feynman, in *Feynman Lectures on Computation*, A. J. G. Hey and R. W. Allen, Eds. (Addison-Wesley, Reading, MA, 1997), chap. 6.
2. S. Lloyd, *Sci. Am.* **273**, 140 (October 1995).
3. J. Preskill, *Proc. R. Soc. London Ser. A* **454**, 385 (1998).
4. P. W. Shor, *Proceedings of the 35th Annual Symposium Foundations of Computer Science*, S. Goldweser, Ed. (IEEE Computer Society, Los Alamitos, CA, 1994), pp. 124–134.
5. L. K. Grover, *Phys. Rev. Lett.* **79**, 325 (1997).
6. J. I. Cirac and P. Zoller, *ibid.* **74**, 4091 (1995).
7. Q. A. C. Turchette, C. J. Hood, W. Lange, H. Mabuchi, H. J. Kimbel, *ibid.* **75**, 4710 (1995).
8. S. A. Lloyd, *Science* **261**, 1569 (1993).
9. D. Loss and D. P. DiVincenzo, *Phys. Rev. A* **57**, 120 (1998).
10. B. E. Kane, *Nature* **393**, 133 (1998).
11. E. Y. Andrei, Ed., *Two Dimensional Electron Systems on Helium and Other Cryogenic Substrates* (Academic Press, New York, 1991).
12. C. C. Grimes *et al.*, *Phys. Rev. B* **13**, 140 (1976).
13. K. Shirahama *et al.*, *J. Low Temp. Phys.* **101**, 439 (1995).
14. L. D. Landau and E. M. Lifschitz, *Quantum Mechanics (Non-Relativistic Theory)* (Pergamon, Elmsford, NY, ed. 3, 1977), p. 145.
15. C. C. Grimes and G. Adams, *Phys. Rev. Lett.* **42**, 795 (1979).
16. M. I. Dykman, *Phys. Status Solidi B* **88**, 463 (1978).
17. G. Saville, J. Goodkind, P. M. Platzman, *Phys. Rev. Lett.* **70**, 1517 (1993).

18. We thank M. Lea, P. Fozoni, A. Dahm, and J. Goodkind for agreeing to actually launch experiments on such systems. We would also like to acknowledge many discussions with A. Mills about quantum computing.

17 February 1999; accepted 10 May 1999

Spontaneous Bubble Domain Formation in a Layered Ferromagnetic Crystal

T. Fukumura,[1]* H. Sugawara,[1]† T. Hasegawa,[2] K. Tanaka,[3]‡ H. Sakaki,[3]§ T. Kimura,[4] Y. Tokura[4,5]

Magnetic domain structure on the surface of the layer-structured ferromagnet $La_{1.4}Sr_{1.6}Mn_2O_7$ was observed in the temperature range from 37 to 97 kelvin with a scanning Hall probe microscope. The sensitivity to temperature of the domain structure changes was large relative to that in conventional ferromagnets. The stable and spontaneous appearance of magnetic bubble domains without an external magnetic field was observed in the neighborhood of 70 kelvin. The phenomenon observed could provide a potential route toward magnetic bubble memory.

The development of the computer industry demands higher density magnetic recording memory, which is being achieved by using smaller magnetic domains. The bubble domain is considered useful as a magnetic bit of high-density magnetic recording memory, because its diameter is small and the circular shape of the bubble domain is stable against any small external disturbance that deforms it (*1*). However, the bubble domain is not widely used for recording memory because the generation of a magnetic domain requires an external magnetic field. The minimization of the sum of the domain wall energy and the magnetostatic energy results in the appearance of a stripe domain instead of a bubble domain unless a magnetic field is applied (*2*). This stripe domain is not completely satisfactory for high-density recording.

We observed a domain structure along the surface of the single crystal of a layered ferromagnetic material, $La_{1.4}Sr_{1.6}Mn_2O_7$, with a scanning Hall probe microscope (SHPM). The domain structure was remarkably different from that of conventional bulk ferromagnetic materials. Small bubble domains formed in the absence of an external magnetic field over a certain temperature range.

Single crystals of $La_{1.4}Sr_{1.6}Mn_2O_7$ were grown by the float-zone method (*3*). This compound has a naturally built-in ferromagnetic multilayer structure regarded as an infinite stacking of magnetic (MnO_2 bilayer) and nonmagnetic layers [$(La,Sr)_2O_2$ layer] and exhibits a marked change in its magnetic structure with temperature (*4, 5*). Recent muon spin rotation (*6*) and neutron diffraction measurements (*7*) have revealed that long-range ferromagnetic coupling within a bilayer evolves below ~90 K, where the magnetic moments begin to rotate toward the *c* axis (perpendicular to MnO_2 bilayers) with decreasing temperature. At temperatures below 60 K, the magnetic moments of respective single MnO_2 layers couple ferromagnetically within a bilayer and align nearly along the *c* axis. The magnetic coupling between the adjacent MnO_2 bilayers is mostly antiferromagnetic.

The cleaved *ab* plane (parallel to MnO_2 bilayers) of a single crystalline platelet sample (2 mm by 1.4 mm by 0.8 mm) was examined under a homemade variable-temperature SHPM (*8*). The SHPM is designed to pick up the spatial distribution of the magnetic field just above the sample surface by scanning a horizontally placed miniature Hall probe. The distribution of the *c*-axis component of the magnetic field, B_z, was imaged by keeping a probe-to-sample distance of ~0.5 μm. The active area of the Hall probe was 1.8 μm by 1.8 μm, and its Hall coefficient was ~1.2 ohm/mT. Under a zero magnetic field, the SHPM measurements were performed from 37 to 97 K. The Hall probe was scanned over the same area throughout the measurements, although the scanned area became narrower as the temperature was lowered because of the reduction of the piezoelectric constant. SHPM images were taken at various temperatures (Fig. 1).

At 37 K, the observed B_z was approximately zero over most of the scanned area (Fig. 1A), representing the disappearance of net magnetization due to antiferromagnetic coupling between adjacent MnO_2 bilayers; that is, the magnetization of the adjacent bilayers is opposite each other, yielding zero magnetic field above the sample surface. However, magnetic domains were observed on the right-hand side of the image. At 51 K, these ferromagnetic domains occupied nearly half of the imaged area (Fig. 1C). As temperature was increased, the area of the domains expanded, accompanied by the increase in B_z. These images (Fig. 1, A to C) indicate the existence of ferromagnetic coupling between the adjacent MnO_2 bilayers, as well as the antiferromagnetic coupling.

At 60 K, a multidomain structure appeared throughout the imaged area with a domain size of ~3 μm (Fig. 1D). The domains had an elongated shape and were ar-

[1]Department of Applied Chemistry, University of Tokyo, Tokyo 113-8656, Japan. [2]Materials and Structures Laboratory, Tokyo Institute of Technology, Yokohama 226-8503, Japan. [3]Research Center for Advanced Science and Technology, University of Tokyo, Tokyo 153-8904, Japan. [4]Joint Research Center for Atom Technology, Tsukuba 305-0046, Japan. [5]Department of Applied Physics, University of Tokyo, Tokyo 113-8656, Japan.

*To whom correspondence should be addressed. Present address: Department of Innovative and Engineered Materials, Tokyo Institute of Technology, Yokohama 226-8502, Japan. E-mail: fukumura@oxide.rlem.titech.ac.jp

†Present address: Department of Electronic Systems Engineering, Tokyo Metropolitan Institute of Technology, Tokyo 191-0065, Japan.

‡Present address: Department of Physical Electronics, Hiroshima University, Higashihiroshima 739-8526, Japan.

§Present address: Institute of Industrial Science, University of Tokyo, Tokyo 106-8558, Japan.